

Modeling and simulation of the injection of urea-water-solution for automotive SCR DeNO_x-systems

Felix Birkhold^{a,*}, Ulrich Meingast^a, Peter Wassermann^a,
Olaf Deutschmann^b

^a Robert Bosch GmbH, Robert-Bosch-Platz 1, 70049 Stuttgart, Germany

^b Institute for Chemical Technology and Polymer Chemistry,
University of Karlsruhe, 76131 Karlsruhe, Germany

Available online 30 June 2006

Abstract

The evaporation of water from a single droplet of urea water solution is investigated theoretically by a Rapid Mixing model and a Diffusion Limit model, which also considers droplet motion and variable properties of the solution. The Rapid Mixing model is then implemented into the commercial CFD code Fire 8.3 from AVL Corp. Therein, the urea water droplets are treated with Lagrangian particle tracking. The evaporation model is extended for droplet boiling and thermal decomposition of urea. CFD simulations of a SCR DeNO_x-system are compared to experimental data to determine the kinetic parameters of the urea decomposition. The numerical model allows to simulate SCR exhaust system configurations to predict conversion and local distribution of the reducing agent.

© 2006 Elsevier B.V. All rights reserved.

Keywords: Evaporation; Thermal decomposition; Urea-water-solution; Simulation; Injection; CFD; SCR; NO_x

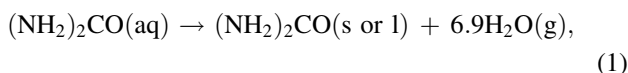
1. Introduction

Selective catalytic reduction (SCR) of NO_x is an effective technique for the reduction of nitrogen oxides emitted from various sources. In automotive applications, the urea-water-solution based SCR is a promising method for control of NO_x emissions.

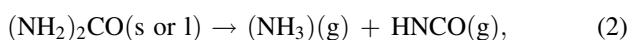
Urea-water-solution (UWS, contains 32.5 wt.% urea; brand name: AdBlue) is sprayed into the hot exhaust stream [1].

The subsequent generation of NH₃ in the hot exhaust gas proceeds in three steps [2,3]:

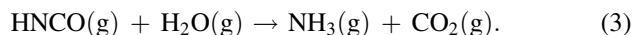
(i) evaporation of water from a fine spray of UWS droplets,



(ii) thermolysis of urea into ammonia and iso-cyanic acid,



(iii) and hydrolysis of isocyanic acid,



As the evaporation and spatial distribution of the reducing agent upstream the catalyst are crucial factors for the conversion of NO_x, the dosing system has to ensure the proper preparation of the reducing agent at all operating conditions. Table 1 gives an overview of the different exhaust gas and spray characteristics occurring in passenger cars and trucks. Appropriate spray properties of the urea solution will also avoid deposition of urea on walls, which could lead to melamine complexes [4].

To our knowledge, there are no studies published on the influence of urea on the evaporation of water from a UWS droplet. Van Helden et al. [5] used water instead of UWS in a CFD study and estimated the concentration of the reducing agent from the water vapor concentration. Wurzenberger and Wanker [6] modeled the thermal decomposition as a homogeneous gas phase reaction, which followed the evaporation of UWS to water vapor and gaseous urea. Chen and Williams [7] and Deur et al. [8] assumed the thermal decomposition to occur

* Corresponding author. Tel.: +49 811 41659; fax: +49 811 262203.

E-mail address: felix.birkhold@de.bosch.com (F. Birkhold).

Nomenclature

a	thermal conductivity, m^2/s
A	frequency factor, $\text{kg}/\text{s m}$
$B_{M,T}$	Spalding numbers
c	molar concentration, mol/m^3
c_p	heat capacity, $\text{J}/\text{kg K}$
D	diameter, m
E_a	activation energy, J/mol
h	specific enthalpy, J/kg
H	molar enthalpy, J/mol
Le	Lewis number
m	mass, kg
\dot{m}	mass flow, kg/s
Nu	Nusselt number
P	pressure, Pa
r	radius, m
r	rate of reaction, $\text{mol}/\text{m}^3 \text{ s}$
R	universal gas constant, $\text{J}/\text{mol K}$
Sh	Sherwood number
t	time, s
T	temperature, K
u	velocity, m/s
v	volume fraction
w	dimensionless radius, r/r_d
Y	mass fraction

Greek symbols

λ	heat conductivity, $\text{W}/\text{m K}$
ρ	density, kg/m^3
Γ	diffusion coefficient, m^2/s

Subscripts

0	initial
*	characteristic
∞	ambient
d,g	droplet, gas
hy	hydrolysis
l,vap	liquid, vapor
u	urea
ref	reference
rel	relative
s	droplet surface
th	thermolysis

instantaneously relative to the evaporation rate. Kim et al. [9] used a single kinetic rate de-volatilization model neglecting the appearance of isocyanic acid. Cremer et al. [10] assumed a fast decomposition of urea after the evaporation of pure water, because their focus was the selective non-catalytic reaction with temperatures above 1100 K.

Analyzing the literature it does not seem to be clear in which state of aggregation urea appears after the evaporation of water and during the thermal decomposition. Yim et al. [2] indicated liquid or gaseous urea, Schaber et al. [11,12] reported that molten urea evaporates to gaseous urea at temperatures above

Table 1

Exhaust gas properties and spray parameters for urea dosing system using UWS in automotive applications

Exhaust	
Exhaust velocity	5–100 m/s
Exhaust temperature	400–1000 K
Wall temperature	350–900 K
Spray	
Sauter mean diameter	20–150 μm
Injection velocity	5–25 m/s
Injection temperature	300–350 K

413 K, but mainly decompose directly to NH_3 and HNCO above 425 K. Schmidt [13] excluded the existence of molten urea when urea particles are exposed to temperatures above 553 K in a fluidized bed reactor. Koebel et al. [3] revealed that atomization of UWS in hot exhaust stream yields to solid or molten urea. The relevance of the physical condition of urea depends on the different inertia and tracking of gaseous and solid/molten urea in the gas stream and the differences in enthalpy. It is essential to know about spatial enthalpy variations due to evaporation, thermolysis, and hydrolysis, which will be discussed in this article.

As the behavior of an UWS droplet in a heated environment is presently not well understood, a theoretical investigation of the evaporation of UWS droplets is presented. Differences in the evaporation between UWS and water are shown and a model to describe the thermal decomposition of urea is developed. The model containing both evaporation of water and the following thermal decomposition of urea is implemented into the CFD code Fire v8.3 [14]. The kinetic parameters for the decomposition model are determined comparing numerical simulation with experimental data from Kim et al. [9]. The model derived in the present study allows to judge different SCR exhaust system configurations with respect to conversion and local distribution of reducing agent. Furthermore the behavior of droplets which impinge on the walls or catalyst can be estimated, because the physical conditions such as temperature and urea concentration of the droplets are determined from the simulation.

2. Evaporation of urea-water-solution droplet

The influence of urea on the evaporation of water from a UWS droplet is investigated theoretically by different evaporation models considering droplet motion and variable properties of UWS and the ambient gas phase.

2.1. Liquid phase

To evaluate the influence of solved urea on the evaporation of water, three different evaporation models are used:

- Rapid Mixing model (RM model): Within the RM model infinite high transport coefficients are assumed for the liquid phase, resulting in spatial uniform temperature, concentration and fluid properties in the droplet, but the quantities will

change in time [15,16]. The variation of urea concentration of the droplet can be evaluated by

$$\frac{dY_u}{dt} = -\frac{\dot{m}_{\text{vap}}}{m_d} Y_u. \quad (4)$$

Mass flow from liquid to gaseous phase is defined to be negative.

- Diffusion Limit model (DL model): Neglecting internal convection only diffusive transport of energy and mass are assumed. The diffusion equation for species and energy in the droplet is solved, considering variable fluid properties [17]:

$$\frac{\partial Y_u}{\partial t} = \frac{\Gamma_u}{r_d^2} \left[\frac{\partial^2 Y_u}{\partial w^2} + \left(\frac{2}{w} + \frac{1}{\rho_d} \frac{\partial \rho_d}{\partial w} + \frac{1}{\Gamma_u} \frac{\partial \Gamma_u}{\partial w} + \frac{r_d}{\Gamma_u} \left(w \frac{dr_d}{dt} - u_r \right) \right) \frac{\partial Y_u}{\partial w} \right] \quad (5)$$

$$\frac{\partial T_d}{\partial t} = \frac{a_d}{r_d^2} \left[\frac{\partial^2 T_d}{\partial w^2} + \left(\frac{2}{w} + \frac{1}{\lambda_d} \frac{\partial \lambda_d}{\partial w} + \frac{r_d}{a_d} \left(w \frac{dr_d}{dt} - u_r \right) \right) \frac{\partial T_d}{\partial w} \right] \quad (6)$$

with

$$a_d = \frac{\lambda_d}{\rho_d c_{p,d}}. \quad (7)$$

u_r denotes a radial convective velocity which accounts for the variable density field within the droplet. The derivation of this approach has been described in detail by Schramm [18].

- Effective Diffusion model (ED model): The ED model accounts for internal circulation due to forced convection. It is based on the DL model and additionally considers internal circulation by an empirical correction of the transport coefficients Γ_u and λ_d [19].

The RM and DL models describe the physical limits of infinite high and only diffusive transport. It can be assumed that the real droplet behavior is within the range of their solutions.

As the temperature and the urea concentration change strongly during evaporation it is obvious to use variable fluid properties. In Table 2 the sources for the used correlations applied for the liquid fluid are summarized. For the calculations it is additionally assumed that no crystallization of urea occurs. The droplets are assumed to be spherical throughout the evaporation and decomposition processes.

Table 2
Thermophysical properties of liquid phase

Property	Correlation
Density	Perman and Lovett [20]
Heat capacity	Gmelin [21]
Dynamic viscosity	Jaeger et al. [22]
Thermal conductivity	VDI-Wärmeatlas [23]
Enthalpy of evaporation	VDI-Wärmeatlas [23]
Diffusion coefficient	Longworth [24], Gmelin [21]

2.2. Phase change

The water vapor concentration on the droplet surface is influenced by the surface urea concentration. This vapor concentration has a decisive impact on the evaporation. For the calculations the correlation from Perman and Lovett [20] is used. The evaporation enthalpy is taken for pure water, because our measurements with UWS show no significant deviation from the values for water given in literature [23].

2.3. Gas phase

For the gas phase the quasi-steady model [15] is used. This approach is suitable to describe the evaporation process in the range of the present conditions even in a free convection situation [25] using the 1/3-rule [26] for the reference values for fluid properties. Integration of the transport equations for mass and enthalpy outside the droplet yields analytical expressions for the diffusive transport fluxes. The differential equations for droplet mass and temperature can be derived from mass and energy balances [19,15]

$$\frac{dm_d}{dt} = -\pi D_d \rho_{g,\text{ref}} \Gamma_{g,\text{ref}} \text{Sh}^* \ln(1 + B_M) \quad (8)$$

$$\frac{dT_d}{dt} = -\frac{\dot{m}_{\text{vap}}}{m_d c_{p,d}} \left(\frac{c_{p,\text{vap,ref}} (T_g - T_d)}{B_T} - h_{\text{vap}} \right) \quad (9)$$

The Spalding heat and mass transfer numbers B_M and B_T are calculated as

$$B_M = \frac{Y_{\text{vap,s}} - Y_{\text{vap,g}}}{1 - Y_{\text{vap,s}}} \quad (10)$$

and

$$B_T = (1 + B_M)^x - 1, \quad x = \frac{c_{p,\text{vap,ref}} \text{Sh}^*}{c_{p,g,\text{ref}} \text{Nu}^* \text{Le}} \quad (11)$$

If boiling temperature is reached during the evaporation, it is assumed that the droplet remains at this temperature. Thus the evaporating mass can be determined from

$$\frac{dm_d}{dt} = -\pi D_d \frac{\lambda_{g,\text{ref}}}{c_{p,\text{vap,ref}}} \text{Nu}^* \ln(1 + B_T) \quad (12)$$

with

$$B_T = \frac{c_{p,\text{vap,ref}} (T_g - T_s)}{h_{\text{vap}}} \quad (13)$$

The approach accounts for non-unit Lewis number and the effect of Stefan flow on heat and mass transfer. Convective transport is considered by a modified Sherwood and Nusselt number using the well-established Frossling correlations [27].

3. Thermal decomposition of urea particle

Urea melts at 406 K [28] and the thermal decomposition of urea into ammonia and isocyanic acid [Eq. (2)] starts. Thermolysis becomes fully evident above 425 K [29,12].

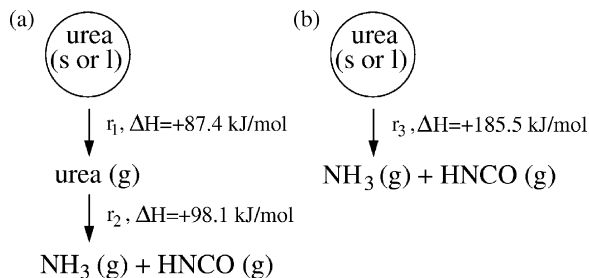


Fig. 1. Two possible ways for thermal decomposition of an urea particle with reaction rates r_i and corresponding enthalpies ΔH (denoted for solid urea, at standard conditions, 298 K and 1 bar): with gaseous urea (a) and without gaseous urea (b).

The RM model, describing the evaporation, is extended to calculate the following thermal decomposition of urea.

From literature two different ways for the thermal decomposition can be derived, as outlined in Fig. 1:

- (a) evaporation of molten/solid urea to gaseous urea, which decomposes in the gas phase into NH₃ and HNCO or
- (b) the direct way from molten/solid urea to gaseous NH₃ and HNCO.

These two ways differ mainly in the way how the heat of the reaction is provided. Furthermore, the inertia and thus the particle tracking of solid or molten urea is quite different to the behavior of gaseous urea in the exhaust stream. In the first case, the sublimation enthalpy of +87.4 kJ/mol (at standard conditions, 298 K and 1 bar) yields a cooling of the particle (reaction rate r_1), whereas the following decomposition (r_2) with an enthalpy consumption of +98.1 kJ/mol results in a direct decrease of the gas phase temperature.

The results shown below reveal, that the thermal decomposition of urea is limited by kinetics. Thus, urea must be present for a certain time during decomposition in the solid/liquid or gaseous state. But gaseous urea does not seem to be stable at elevated temperatures, because there is no report on the presence of gaseous urea. Therefore, we assume a very fast reaction from gaseous urea to NH₃ and HNCO for the first case ($r_2 \gg r_1$). Thus, if this reaction occurs, it takes place in the boundary layer of the particle only. The enthalpy change due to evaporation of solid urea and reaction of gaseous urea is +185.5 kJ/mol in total and has to be transported to the particle surface via the boundary layer.

Hence, we have the same situation concerning heat transfer as in the second way where the complete reaction enthalpy of thermolysis of +185.5 kJ/mol affects the particle (r_3). From energetic aspects it is not important if urea melts first or not, since molten urea likely remains spherical, resulting in the same heat transfer condition. We modeled the direct decomposition from solid/molten urea to NH₃ and HNCO and simply included the melting process with the modest urea melting enthalpy of +14.5 kJ/mol in the thermolysis.

As there is no reasonable condition for the phase change of urea, an alternative way as used for the evaporation of water must be taken to calculate the decomposition rate:

For the description of the decomposition an extended Arrhenius expression is used,

$$\frac{dm_u}{dt} = -\pi D_d A e^{(-E_a/RT_d)} \quad (14)$$

The heat transfer to the particle is calculated using

$$q_d = \pi D_d \lambda_{g,\text{ref}} \text{Nu}^* (T_g - T_d) + \frac{dm_u}{dt} h_{\text{th}} \quad (15)$$

as a result of heat balance.

4. Modeling of of urea-water-solution spray

For the calculation of the injection of UWS, the models for evaporation and thermal decomposition are implemented into the CFD code Fire v8.3 from AVL [14]. In Fire the UWS droplets are treated with Lagrangian particle tracking, which solves the equation of motion for parcels of droplets with identical properties using the Discrete Droplet Method of Dukowicz [30]. Turbulence dispersion is defined by the Eddy-Lifetime model [31]. Between droplets and gas phase two-way coupling is considered for momentum, mass and heat. For turbulence kinetic energy and dissipation one-way coupling is applied.

Hydrolysis of HNCO [Eq. (3)] is considered as a homogeneous gas phase reaction using the coupling interface of Fire to the CHEMKIN chemistry solver [32].

5. Results and discussion

5.1. Evaporation modeling

When UWS is atomized into a hot gas stream, the droplets are heated up and, due to the low vapor pressure of urea compared to the vapor pressure of water [21], water evaporates first from the droplets. The evaporation of water leads to a spatial urea concentration gradient with a maximum at the droplet surface. Convection and diffusion smooth out the concentration gradients inside the droplet. Thus solved urea at the droplet surface causes a decrease of the vapor pressure of the water. This effect is heightened during the evaporation. The

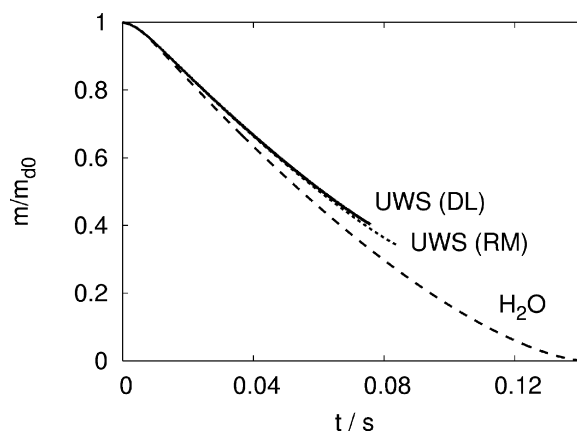


Fig. 2. Decrease of droplet mass. Conditions: $D_{d0} = 70 \mu\text{m}$, $T_{d0} = 300 \text{ K}$, $T_\infty = 673 \text{ K}$, $u_{\text{rel}} = 0 \text{ m/s}$, $p = 0.11 \text{ MPa}$. Calculations stopped at $T_s = 373 \text{ K}$.

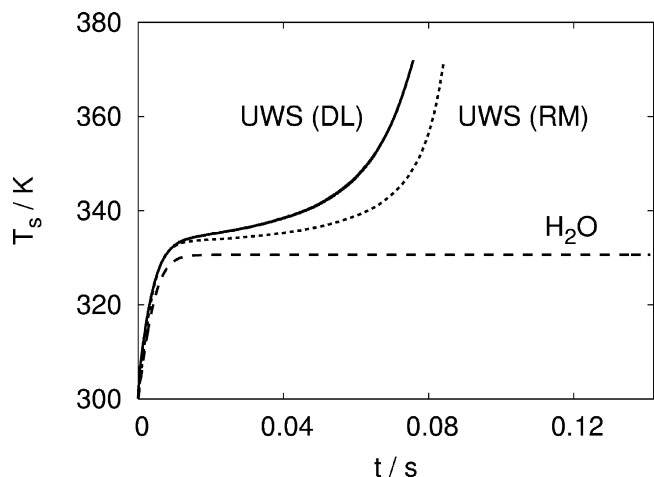


Fig. 3. Droplet surface temperature during evaporation for H₂O and UWS droplet: effect of vapor pressure change due to increase of urea surface concentration, predicted by different models. Conditions: $D_{d0} = 70 \mu\text{m}$, $T_{d0} = 300 \text{ K}$, $T_{\infty} = 673 \text{ K}$, $u_{\text{rel}} = 0 \text{ m/s}$, $p = 0.11 \text{ MPa}$. Calculations stopped at $T_s = 373 \text{ K}$.

decrease of vapor pressure results in a lower evaporation rate [33]. Fig. 2. shows the slower decrease of droplet mass during the evaporation for UWS compared to pure water. For UWS both models DL and RM predict a similar mass change, with a little smaller rate for the DL model.

The results for the droplet surface temperature are depicted in Fig. 3. While the temperature of a water droplet remains constant after the heating period the UWS droplet surface temperature increases continuously. The decrease of vapor pressure at the UWS droplet yields a smaller evaporation rate. Identical heat transfer to the droplet and less cooling due to evaporation enthalpy at UWS results in an increase of droplet temperature and therefore vapor pressure. But as the droplet temperature rises, the heat transfer decreases, because the temperature difference,

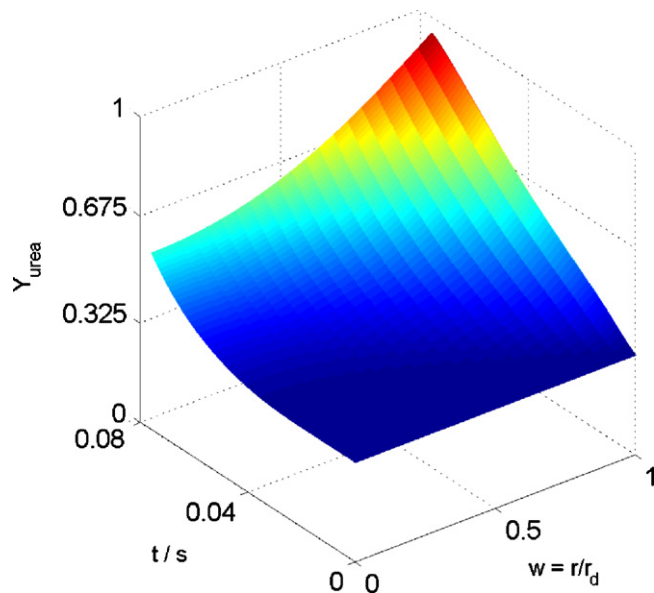


Fig. 4. Urea concentration during evaporation, predicted with DL model. Conditions: $D_{d0} = 70 \mu\text{m}$, $T_{d0} = 300 \text{ K}$, $T_{\infty} = 673 \text{ K}$, $u_{\text{rel}} = 0 \text{ m/s}$, $p = 0.11 \text{ MPa}$.

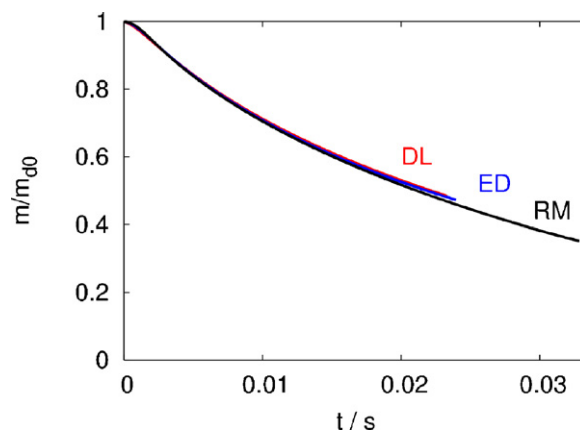


Fig. 5. Comparison of evolution of UWS droplet mass with DL, ED and RM model with forced convection at elevated temperature. Conditions: $D_{d0} = 70 \mu\text{m}$, $T_{d0} = 300 \text{ K}$, $T_{\infty} = 900 \text{ K}$, $u_{\text{rel}} = 100 \text{ m/s}$, $p = 0.11 \text{ MPa}$. Calculations stopped at $T_s = 373 \text{ K}$.

$T_g - T_s$, decreases. Slower evaporation as shown in Fig. 2 is the result. For UWS a difference between DL and RM model in the heating behavior of the droplet is observed. However, there is no significant difference in the evolution of droplet mass, although the DL model predicts concentration gradients. Fig. 4 shows the time evolution of the urea concentration inside the droplet, from the center ($w = 0$) to the surface of the droplet ($w = 1$). Since the characteristic heating time $t \sim r_d^2/a_d \approx 7 \times 10^{-3} \text{ s}$ is much shorter than the evaporation time no significant gradients in droplet temperature appear.

For a droplet in a free convection situation the RM and DL models predict almost the same evaporation rates. The strongest influence of diffusion resistance inside the droplet is expected at elevated ambient temperature and forced convection, because both yield in high evaporation rates. So the different evaporation models, including the ED model, are tested for UWS at these conditions. Fig. 5 shows the decrease in droplet mass for the three evaporation models for an ambient temperature of 900 K and a relative velocity of 100 m/s.

As expected the result for the ED model is between the prediction of RM and DL model; as in the free convection situation, there is no significant difference between the models.

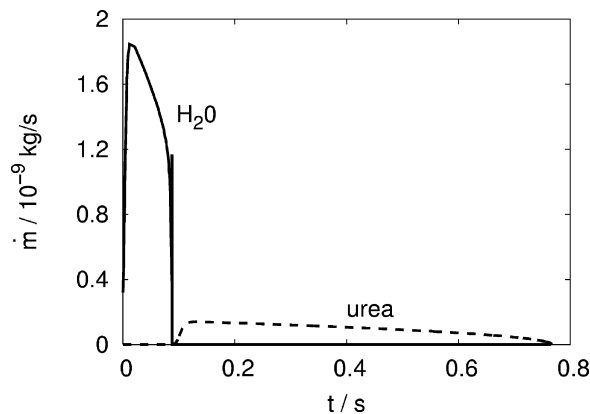


Fig. 6. Mass flow for water vapor and urea during evaporation and decomposition. Conditions: $D_{d0} = 70 \mu\text{m}$, $T_{d0} = 300 \text{ K}$, $T_{\infty} = 673 \text{ K}$, $u_{\text{rel}} = 0 \text{ m/s}$, $p = 0.11 \text{ MPa}$, $A = 0.42 \text{ kg/sm}$, $E_a = 6.9 \times 10^4 \text{ J/mol}$.

Without the need of discretization of the droplet interior and without a time consuming solution of transport equation, the RM model is a numerically effective method to predict the evaporation of water from UWS droplets. Since it is based on algebraic equations, about 10 times less computational time is required compared to the DL and ED model.

The results reveal that the RM model for UWS is suitable for the use in a multi-phase CFD code and a good compromise between accuracy and numerical effort. In technical applications, the calculation of a few thousand droplet packages is usually needed to simulate realistic spray propagation.

5.2. Thermal decomposition

After the evaporation of water urea melts at 406 K and thermal decomposition starts. In Fig. 6 the calculated mass fluxes of water vapor and urea due to evaporation and decomposition are shown. The evaporation mass flow increases as the droplet heats up and decreases as the droplet diameter decreases. The small peak at the end of the evaporation occurs when boiling temperature is reached since the droplet temperature remains constant. The decomposition of urea occurs at lower rates than the evaporation of water. This is a combination of the higher particle temperature and thus a lower heat transfer, the higher reaction enthalpy ($h_{th} \approx 3088$ kJ/kg $>$ 2300 kJ/kg $\approx h_{vap}$) and the limiting kinetic.

The model for the decomposition rate [Eq. (14)] results in a constant particle temperature during decomposition since both convective heat transfer to the droplet and decomposition rate are proportional to the droplet diameter. As the decomposition temperature and thus the rate increases, the heat transfer to the particle decreases, until transferred heat and enthalpy of decomposition are balanced. Fig. 7 shows the evolution of the droplet/particle temperature during the evaporation and decomposition process. We can assume that the urea is molten since the particle stays for a certain time at a temperature above the melting temperature of 406 K.

Fig. 8 depicts the associated D^2 -ratio with the different slopes for evaporation and decomposition.

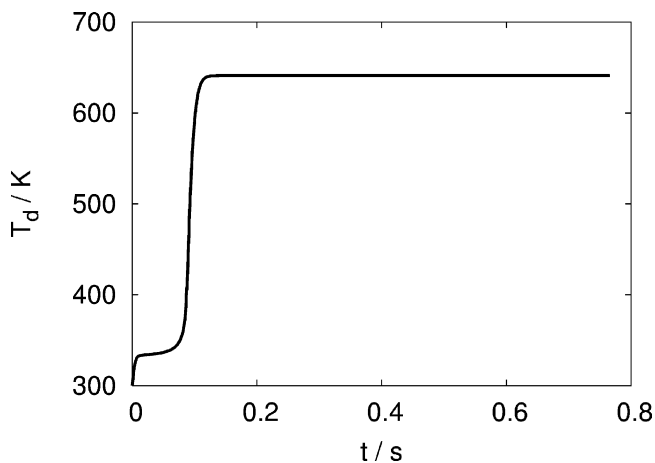


Fig. 7. Droplet/particle temperature during evaporation and decomposition. Conditions: $D_{d0} = 70$ μ m, $T_{d0} = 300$ K, $T_{\infty} = 673$ K, $u_{rel} = 0$ m/s, $p = 0.11$ MPa, $A = 0.42$ kg/sm, $E_a = 6.9 \times 10^4$ J/mol.

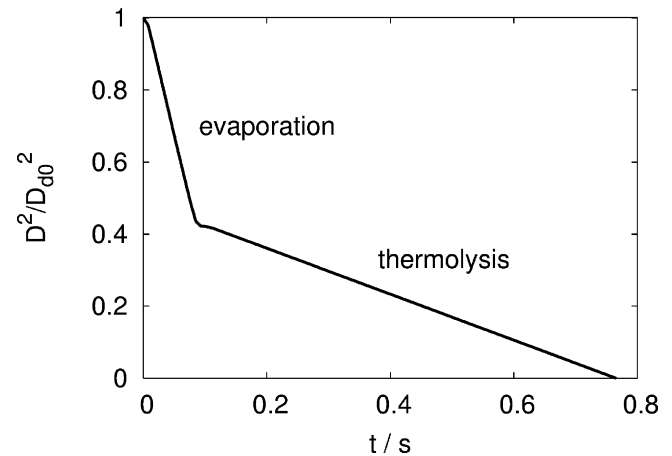


Fig. 8. Evolution of squared droplet diameter: change of slope after complete evaporation of water due to higher reaction enthalpy compared to evaporation enthalpy of water. Conditions: $D_{d0} = 70$ μ m, $T_{d0} = 300$ K, $T_{\infty} = 673$ K, $u_{rel} = 0$ m/s, $p = 0.11$ MPa, $A = 0.42$ kg/sm, $E_a = 6.9 \times 10^4$ J/mol.

5.3. Simulation of urea-water-solution-injection

To evaluate the Arrhenius parameters of the decomposition [Eq. (14)] the simulation is compared to an experimental investigation of Kim et al. [9] studying the conversion from injected UWS to ammonia. The UWS (here a solution with 40 wt% urea is used) was directly injected at the axis of a tube (Fig. 9) at gas temperatures of 573 K, 623 K and 673 K and average velocities varying from 6.0 to 10.8 m/s. The average conversion rates were measured at distances of 3 m, 4.5 m and 6 m downstream the injection, yielding to residence times between 0.3 s and 1.0 s.

The droplets are initialized with a Rosin-Rammler distribution

$$v(D) = 1 - e^{-(D^{3.27}/44)} \quad (16)$$

an injection velocity of 10.6 m/s and an UWS flow rate of 3.3×10^{-4} kg/s.

The rate of hydrolysis of HNCO [Eq. (3)] is given by Yim et al. [2] by

$$r_{hy} = c_{HNCO} 2.5 \times 10^5 e^{(-62220/RT)}. \quad (17)$$

Evaporation and thermolysis of the droplets is calculated using the RM model. The kinetic parameters of the thermal decomposition, frequency factor A and activation energy E_a [Eq. (14)] are fitted to match the experimental data using least squares method. The activation energy of 7.3×10^4 J/mol proposed by

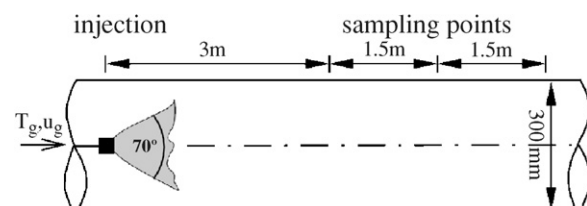


Fig. 9. Sketch of the experimental setup of Kim et al. [9] (not to scale).

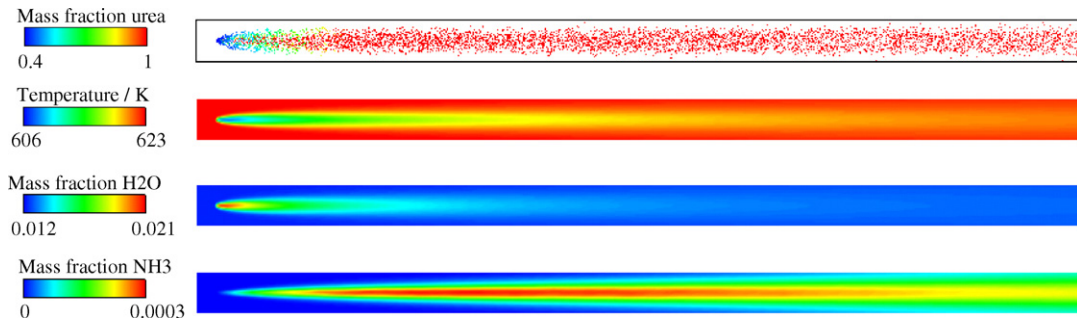


Fig. 10. Numerical results of spray propagation (the droplets are colored with urea fraction), gas temperature, water vapor concentration and NH_3 concentration in gas phase ($T_g = 623 \text{ K}$, $u_g = 9.1 \text{ m/s}$).

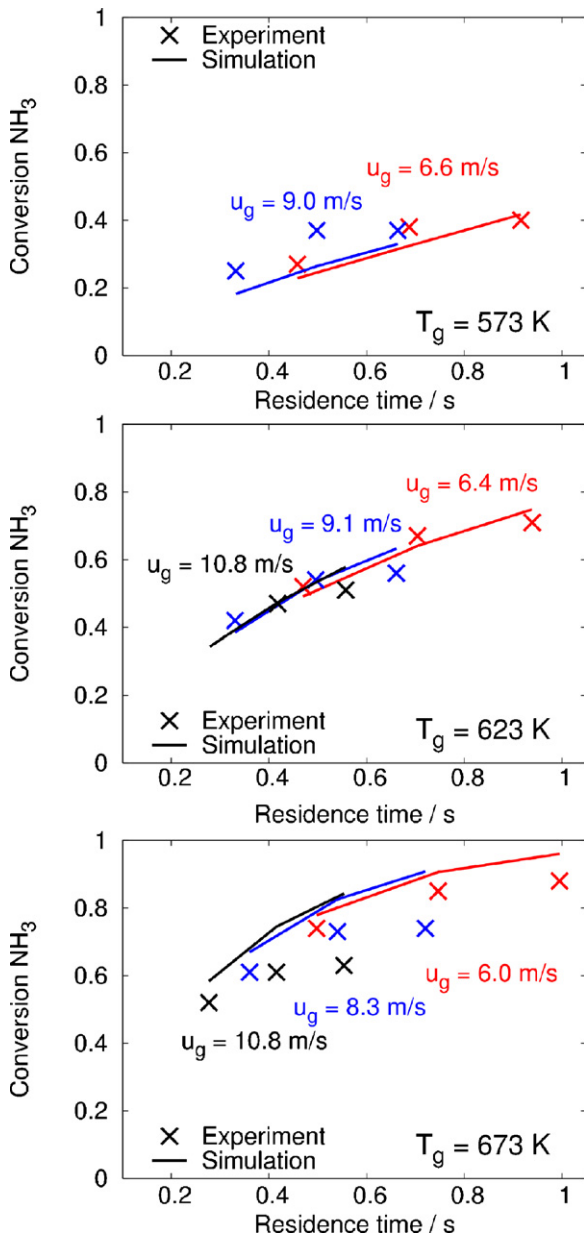


Fig. 11. Calculated conversion to NH_3 for different gas velocities and gas temperatures compared to experimental data of Kim et al. [9].

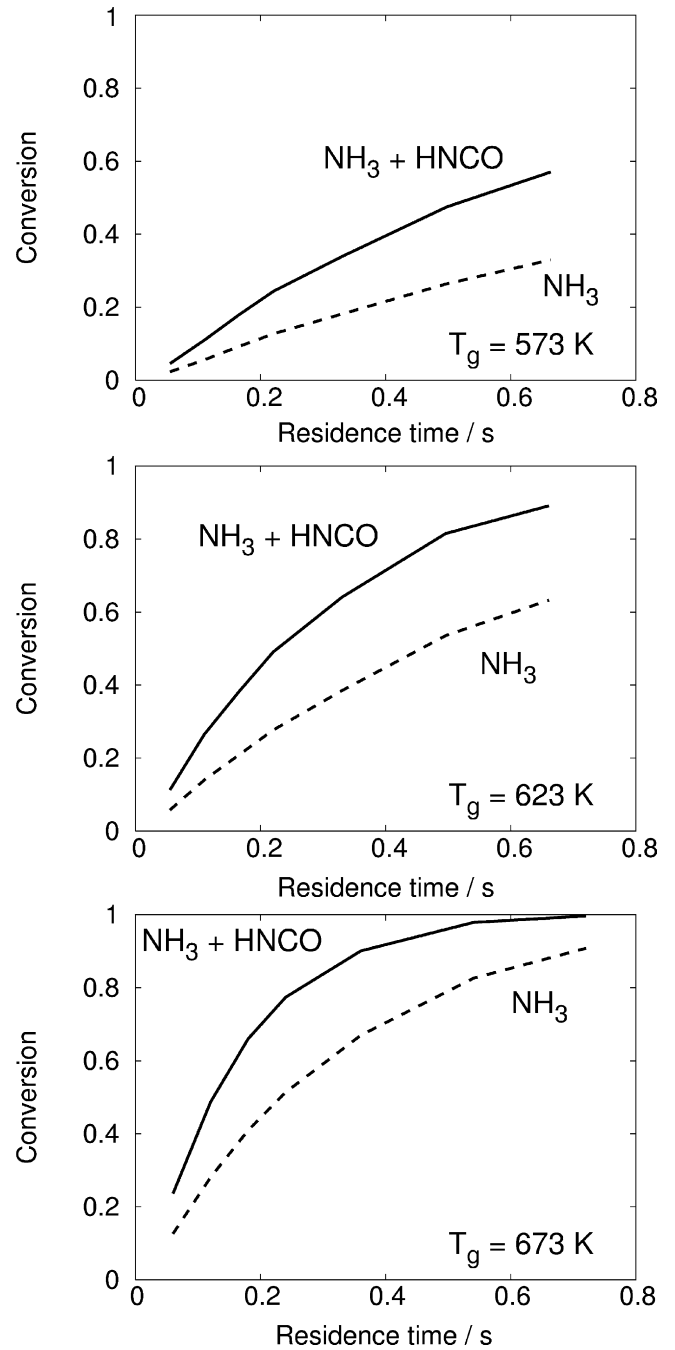


Fig. 12. Predicted conversion to NH_3 and NH_3 equivalent at different gas temperatures.

Buchholz [34] is used as initial guess. The fitting procedure yields

$$\begin{aligned} A &= 0.42 \text{ kg/sm} \\ E_a &= 6.9 \times 10^4 \text{ J/mol.} \end{aligned} \quad (18)$$

Fig. 10 exemplarily depicts the results of the numerical calculation for $T_g = 623 \text{ K}$ and $u_g = 9.1 \text{ m/s}$. Small droplets show a minor radial penetration and evaporate and decompose faster than the bigger droplets. Therefore, the main drop in temperature and the maximum concentrations of water vapor and NH_3 appear in the middle part of the tube. While the highest water vapor concentrations occur near the nozzle the production of NH_3 occurs further downstream due to the kinetic of the thermal decomposition.

Fig. 11 shows the calculated urea conversion to NH_3 compared to the experimental data for $T_g = 573 \text{ K}$, $T_g = 623 \text{ K}$, $T_g = 673 \text{ K}$ and varying average gas velocity. Conversion is defined as the ratio of the amount of NH_3 measured or calculated to the maximum concentration when urea is transformed completely into NH_3 .

The simulations agree well with the experimental data at 623 K . While at 573 K the calculation underestimates the experiment the simulation predicts slightly higher conversion rates at 673 K . One should consider that the conversion to NH_3 is a result from both thermal decomposition of urea and hydrolysis of HNCO in the gas phase. Uncertainties could occur in the description of both reactions. The hydrolysis reaction does not occur significantly at temperatures below 573 K [9]. So conversion at this temperature is only due to thermal decomposition resulting in approximately the same amount of both gaseous products at all positions. Fig. 12 shows the calculated conversion to NH_3 and HNCO at varying gas temperature as a function of the residence time. At 673 K most of the HNCO is already hydrolyzed at the highest residence times. The decrease of conversion rate with increasing residence time is due to slow evaporation and thermolysis of large droplets. This effect is pronounced at high temperatures.

6. Conclusions

The influence of urea on the evaporation of urea water solution has been studied. The decrease in vapor pressure due to increasing concentration of urea in the droplet results in a continuous increase of the droplet temperature and a slower evaporation compared to pure water. Describing the evaporation process with different physical models, the Diffusion Limit model predicts a higher urea concentration at the surface than the Rapid Mixing model due to gradients in the droplet. Nevertheless the Diffusion Limit and Rapid Mixing models predict a similar variation in droplet diameter during evaporation at exhaust conditions.

The Rapid Mixing model has been extended to describe the thermal decomposition of urea using an Arrhenius formulation after the evaporation of water is completed. The kinetic parameter for the decomposition has been determined by comparing numerical CFD simulations with experimental data from Kim et al. [9]. The results agree sufficiently.

The CFD model predicts the urea concentration and the temperature of the urea water solution droplets and urea particles, which is important for the understanding of their impingement on catalyst and wall. Furthermore, the conversion into gaseous reducing agents, NH_3 and HNCO , serves as boundary condition for dimensioning of the catalytic converter, in which the reduction of the nitrogen oxides by ammonia will be conducted.

The results reveal that in real exhaust configurations the urea water solution does not evaporate and decompose completely. The catalyst must have a sufficient capability for the hydrolysis reaction, especially at temperatures below 573 K , at which no significant hydrolysis in the gas phase occurs. Catalyst or surfaces of the exhaust gas system will be important parts for spray mixing and reducing agent preparation.

Acknowledgements

We gratefully acknowledge the discussion with Hee Je Seong and Seung Hyup Ryu from Hyundai Heavy Industries Co., Ltd.

References

- [1] M. Koebel, M. Elsener, T. Marti, NO_x -reduction in diesel exhaust gas with urea and Selective Catalytic Reduction, *Comb. Sci. and Techn.* 121 (1996) 85–102.
- [2] D.S. Yim, S.J. Kim, J.H. Baik, I. Nam, Y.S. Mok, J.W. Lee, B.K. Cho, S.H. Oh, Decomposition of Urea into NH_3 for the SCR Process, *Ind.Eng.-Chem.Res.* 43 (1) (2004) 4856–4863.
- [3] M. Koebel, M. Elsener, M. Kleemann, Urea-SCR: a promising technique to reduce NO_x emissions from automotive diesel engines, *Catalysis Today.* 59 (2000) 335–345.
- [4] H.L. Fang, H.F.M. DaCosta, Urea thermolysis and NO_x reduction with and without SCR catalysts, *Applied Catalysis B: Environmental* 46 (2003) 17–34.
- [5] R. van Helden, R. Verbeek, F. Willems, Optimization of urea SCR de NO_x Systems for HD Diesel Engines. SAE, 2004-01-0154, 2004.
- [6] J.C. Wurzenberger, R. Wanker, Multi-Scale SCR Modeling, 1D Kinetic Analysis and 3D System Simulation. SAE, 2005-01-0948, 2005.
- [7] M. Chen, S. Williams, Modelling and Optimization of SCR-Exhaust Aftertreatment Systems. SAE, 2005-01-0969, 2005.
- [8] J.M. Deur, S. Jonnavithula, S. Dhanapalan, K. Schulz, B. Raghunathan, H. Nakla, E. Meeks, C.P. Chou, Simulation of Engine Exhaust Aftertreatment with CFD using Detailed Chemistry, in: Proc. 12th International Multi-dimensional Engine Modeling User's Group, Engine Research Center, Detroit, MI, USA, 2002.
- [9] J.Y. Kim, S.H. Ryu, J.S. Ha, Numerical prediction on the characteristics of spray-induced mixing and thermal decomposition of urea solution in SCR system, in: Proc. 2004 Fall Technical Conference of the ASME Internal Combustion Engine Division, Long Beach, California USA, 2004.
- [10] M.A. Cremer, E. Eddings, T. Martz, L.J. Muzio, Q. Quartucy, R. Hardman, J. Cox, J. Stallings, Assessment of SNCR Performance on Large Coal-Fired Utility Boilers. 1998 U.S. DOE Conference on SCR and SNCR for NO_x Control, Pittsburg, PA, 1998.
- [11] P.M. Schaber, J. Colson, S. Higgins, E. Dietz, D. Thielen, B. Anspach, J. Brauer, Study of the urea thermal decomposition (pyrolysis) reaction and importance to cyanuric acid production, American laboratory (1999).
- [12] P.M. Schaber, J. Colson, S. Higgins, D. Thielen, B. Anspach, J. Brauer, Thermal decomposition (pyrolysis) of urea in an open reaction vessel, *Thermochemica Acta* 424 (2004) 131–142.

- [13] A. Schmidt, Verfahrenstechnische Probleme bei der Herstellung von Melamin aus Harnstoff bei Atmosphärendruck, *Österr. Chemiker-Ztg.* 68 (1967) 175–179.
- [14] *FIRE 8.3*. AVL LIST GmbH, A-8020 Graz, Austria, www.avl.com, 2004.
- [15] G.M. Faeth, Evaporation and combustion of sprays, *Prog. Energy Combust. Sci.* 9 (1983) 1–76.
- [16] W.A. Sirignano, Fuel droplet vaporization and spray combustion theory, *Prog. Energy Combust. Sci.* 9 (1983) 291–322.
- [17] R. Kneer, M. Schneider, B. Noll, S. Wittig, Diffusion controlled evaporation of a multicomponent droplet: Theoretical studies on the importance of variable liquid properties, *Int. J. Heat Mass Transfer* 36 (1993) 2403–2415.
- [18] V. Schramm. Erweiterung von Modellansätzen zur numerischen Beschreibung von verdunstenden Sprühstrahlen mit mehreren Flüssigkeitskomponenten. Diplomarbeit, Lehrstuhl und Institut für Thermische Strömungsmaschinen, Universität Karlsruhe, 1997.
- [19] B. Abramzon, W.A. Sirignano, Droplet vaporization model for spray combustion calculations, *Int. J. Heat Mass Transfer*, 32 (1989) 1605–1618.
- [20] E.P. Perman, T. Lovett, Vapour pressure and heat of dilution of aqueous solutions, *Trans. Faraday Soc.* 22 (1926) 1–19.
- [21] Handbuch der anorganischen Chemie: Gmelin. *Deutsche Chemische Gesellschaft*, C,D,1, Verlag Chemie, 1971.
- [22] L. Jaeger, J. Nývlt, S. Horáček, J. Gottfried, Viskositäten von Harnstoffwasserlösungen, *Collection Czech. Chem. Commun.* 30 (1965) 2117–2121.
- [23] VDI-Wärmeatlas, VDI-Gesellschaft, eighth edition, Springer, 1997.
- [24] L.G. Longworth, Temperature dependence of diffusion in aqueous solutions, *J. Phys. Chem.* 58 (1954) 770–773.
- [25] M. Burger, R. Schmehl, P. Prommersberger, O. Schaefer, R. Koch, S. Wittig, Droplet evaporation modeling by the distillation curve model: accounting for kerosine fuel and elevated pressures, *Int. J. Heat Mass Transfer* 46 (2003) 4403–4412.
- [26] E.M. Sparrow, J.L. Gregg, The variable fluid-property problem in free convection, *Trans. ASME* 80 (1958).
- [27] N. Frössling, Über die Verdunstung fallender Tropfen, *Gerlands Beitrag zur Geophysik* 52 (1938) 170–216.
- [28] M. Koebel, M. Elsener, Ammonia production by combined pyrolysis/hydrolysis of urea. *PSI Scientific Report 1992*. 5:50-52, 1993.
- [29] L. Stradella, M. Argentero, A study of the thermal decomposition of urea, of related compounds and thiourea using DSC and TG-EGA, *Thermochimica Acta* 219 (1993) 315–323.
- [30] J.K. Dukowicz, A particle-fluid numerical model for liquid sprays, *Journal of Computational Physics* 35 (1980) 229–253.
- [31] A.D. Gosman, E. Ioannides, Aspects of computer simulation of liquid-fueled com-busters. In *AIAA-81-323*. AIAA, 1981.
- [32] R.J. Kee, F.M. Rupley, E. Meeks, J.A. Miller, Chemkin III: A fortran chemical kinetics package for the analysis of gas-phase chemical and plasma kinetics., Sandia National Laboratories, Livermore, CA 94551-0969, 1996.
- [33] K. Masters, *Spray Drying Handbook*, Longman Scientific Technical, 1991.
- [34] F. Buchholz, Einsatz von festem Harnstoff als Reduktionsmittel für die NO_x-Minderung nach dem SCR-Verfahren. PhD thesis, Fakultät für Chemie, Universität Karlsruhe, 2000.